Characterization of a high coherence, Brillouin microcavity laser on silicon

Jiang Li,[1] **Hansuek Lee,**[1] **Tong Chen, and Kerry J. Vahala***

T. J. Watson Laboratory of Applied Physics,
California Institute of Technology, Pasadena, California 91125, USA
[1] *equal contributors*

*vahala@caltech.edu

Abstract: Recently, a high efficiency, narrow-linewidth, chip-based stimulated Brillouin laser (SBL) was demonstrated using an ultra-high-Q, silica-on-silicon resonator. In this work, this novel laser is more fully characterized. The Schawlow Townes linewidth formula for Brillouin laser operation is derived and compared to linewidth data, and the fitting is used to measure the mechanical thermal quanta contribution to the Brillouin laser linewidth. A study of laser mode pulling by the Brillouin optical gain spectrum is also presented, and high-order, cascaded operation of the SBL is demonstrated. Potential application of these devices to microwave sources and phase-coherent communication is discussed.

OCIS codes: (190.5890) Stimulated; (290.5900) Stimulated Brillouin; (190.4390) Integrated optics.

References and links

1. T. Fortier, M. Kirchner, F. Quinlan, J. Taylor, J. Bergquist, T. Rosenband, N. Lemke, A. Ludlow, Y. Jiang, C. Oates, and S. Diddams, "Generation of ultrastable microwaves via optical frequency division," Nat. Photonics **5**, 425–429 (2011).
2. E. IP, A. Lau, D. Barros, and J. Kahn, "Coherent detection in optical fiber systems," Opt. Express **16**, 753–791 (2008).
3. M. Nakazawa, S. Okamoto, T. Omiya, K. Kasai, and M. Yoshida, "256-QAM (64 Gb/s) coherent optical transmission over 160 km with an optical bandwidth of 5.4 GHz," IEEE Photon. Technol. Lett. **22**, 185–187 (2010).
4. C. Karlsson, F. Olsson, D. Letalick, and M. Harris, "All-fiber multifunction CW coherent laser radar at 1.55 μm for range, speed, vibration, and wind measurements," Appl. Opt. **39**, 3716–3726 (2000).
5. R. Rafac, B. Young, J. Beall, W. Itano, D. Wineland, and J. Berquist, "Sub-dekahertz Ultraviolet Spectroscopy of $^{199}Hg^{+}$", Phys. Rev. Lett. **85**, 2462–2465 (2000).
6. B. Young, F. Cruz, W. Itano, and J. Bergquist, "Visible lasers with aubhertz linewidths," Phys. Rev. Lett. **82**, 3799–3802 (1999).
7. P. Del'Haye, A. Schliesser, O. Arcizet, T. Wilken, R. Holzwarth, and T. J. Kippenberg, "Optical frequency comb generation from a monolithic microresonator," Nature **450**, 1214–1217 (2007).
8. T. J. Kippenberg, R. Holzwarth, and S. A. Diddams, "Microresonator-based optical frequency combs," Science **332**, 555–559 (2011).
9. L. Yang, T. Lu, T. Carmon, B. Min, and K. J. Vahala, "A 4-Hz fundamental linewidth on-chip microlaser," *Conference on Lasers and Electro-Optics* (CLEO), Technical Digest Series (CD) (Optical Society of America, 2007), paper CMR2.
10. T. Lu, L. Yang, T. Carmon, B. Min, and K. J. Vahala, "Frequency noise of a microchip raman laser," *Conference on Lasers and Electro-Optics* (CLEO), Technical Digest Series (CD) (Optical Society of America, 2009), paper CTuB3.
11. W. Liang, V. S. Ilchenko, A. A. Savchenkov, A. B. Matsko, D. Seidel, and L. Maleki, "Whispering-gallery-mode-resonator-based ultranarrow linewidth external-cavity semiconductor laser," Opt. Lett. **35** 2822–2824 (2010).
12. H. Lee, T. Chen, J. Li, K. Yang, S. Jeon, O. Painter, and K. J. Vahala, "Chemically etched ultrahigh-Q wedge-resonator on a silicon chip," Nat. Photonics **6**, 369–373 (2012).

#171557 - $15.00 USD Received 2 Jul 2012; revised 10 Aug 2012; accepted 12 Aug 2012; published 20 Aug 2012

13. S. P. Smith, F. Zarinetchi, and S. Ezekiel, "Narrow-linewidth stimulated Brillouin fiber laser and applications," Opt. Lett. **16** 393–395 (1991).
14. Y. Okawachi, M. Bigelgow, J. Sharping, Z. Zhu, A. Schweinsberg, D. Gauthier, R. Boyd, and A. Gaeta, "Tunable all-optical delays via Brillouin slow light in an optical fiber," Phys. Rev. Lett. **94**, 153902 (2005).
15. I. Grudinin, A. Matsko, and L. Maleki, "Brillouin lasing with a CaF_2 whispering gallery mode Resonator," Phys. Rev. Lett. **102**, 043902 (2009).
16. M. Tomes, and T. Carmon, "Photonic micro-electromechanical systems vibrating at X-band (11-GHz) rates," Phys. Rev. Lett. **102**, 113601 (2009).
17. R. Pant, C. G. Poulton, D. Choi, H. Mcfarlane, S. Hile, E. Li, L. Thevenaz, B. Luther-Davies, S. J. Madden, and B. J. Eggleton, "On-chip stimulated Brillouin scattering," Opt. Express **19**, 8285–8290 (2011)
18. D. K. Armani, T. J. Kippenberg, S. M. Spillane, and K. J. Vahala, "Ultra-high-Q toroid microcavity on a chip," Nature **421**, 925–928 (2003).
19. M. Cai, O. Painter, and K. J. Vahala, "Observation of critical coupling in a fiber taper to silica-microsphere whispering gallery mode system," Phys. Rev. Lett. **85**, 74–77 (2000).
20. S. M. Spillane, T. J. Kippenberg, O. Painter, and K. J. Vahala, "Ideality in a fiber-taper-coupled microresonator system for application to cavity quantum electrodynamics," Phys. Rev. Lett. **91**, 043902 (2003).
21. T. W. Hänsch, and B. Couillaud, "Laser frequency stabilization by polarization spectroscopy of a reflecting reference cavity." Opt. Commun. **35**, 441–444 (1980).
22. A. Schliesser, R. Riviere, G. Anetsberger, O. Arcizet, and T. J. Kippenberg, "Resolved-sideband cooling of a micromechanical oscillator," Nat. Phys. **4**, 415–419 (2008).
23. B. Min, T. J. Kippenberg, and K. J. Vahala, "Compact, fiber-compatible, cascaded Raman laser," Opt. Lett. **28**, 1507–1509 (2003).
24. T. J. Kippenberg, S. M. Spillane, B. Min, and K. J. Vahala, " Theoretical and experimental study of stimulated and cascaded Raman scattering in ultrahigh-Q optical microcavities," IEEE J. Quantum Electron. **10**, 1219–1228 (2004).
25. A. Yariv, *Quantum Electronics* (Wiley, 1989).
26. Z. Wu, L. Zhan, Q. Shen, J. Liu, X. Hu, and P. Xiao, "Ultrafine optical-frequency tunable Brillouin fiber laser based on fiber strain," Opt. Lett. **36**, 3837–3839 (2011).
27. Y. R. Shen and N. Bloembergen, "Theory of stimulated Brillouin and Raman scattering," Phys. Rev. **137**, A1787–A1805 (1965).
28. A. B. Matsko, V. S. Ilchenko, A. A. Savchenkov, and L. Maleki, "Highly nondegenerate all-resonant optical parametric oscillator," Phys. Rev. A **66**, 043814 (2002).
29. I. S. Grudinin, H. Lee, O. Painter and K. J. Vahala, "Phonon laser action in a tunable two-level system," Phys. Rev. Lett. **104**, 083901 (2010) .
30. K. J. Vahala, "Back-action limit of linewidth in an optomechnical oscillator," Phys. Rev. A **78**, 023832 (2008).
31. R. W. Boyd, K. Rzaewski, and P. Narum, "Noise initiation of stimulated Brillouin scattering," Phys. Rev. A **42**, 5514 (1990).
32. A. Debut, S. Randoux, and J. Zemmouri, "Linewidth narrowing in Brillouin lasers: theoretical analysis," Phys. Rev. A **62** 023803 (2000).
33. A. Debut, S. Randoux, and J. Zemmouri, "Experimental and theoretical study of linewidth narrowing in Brillouin fiber ring lasers," J. Opt. Soc. Am. B **18**, 556–567 (2001).
34. M. Okai, M. Suzuki, and T. Taniwatari, "Strained multiquantum-well corrugation-pitch-modulated distributed feedback laser with ultranarrow (3.6 kHz) spectral linewidth," Electron. Lett. **29**, 1696–1697 (1993).
35. M. C. Gross, P. T. Callahan, T. R. Clark, D. Novak, R. B. Waterhouse, and M. L. Dennis, "Tunable millimeter-wave frequency synthesis up to 100 GHz by dual-wavelength Brillouin fiber laser," Opt. Express **18**, 13321–13330 (2010).

1. Introduction

Ultra-high coherence (low frequency noise) is a priority in a remarkably wide range of applications including: high-performance microwave oscillators [1], coherent fiber-optic communications [2, 3], remote sensing [4] and atomic physics [5, 6]. In these applications, the laser forms one element of an overall system that would benefit from miniaturization. For example, in coherent communication systems a laser (local oscillator) works together with taps, splitters and detectors to demodulate information encoded in the field amplitude of another coherent laser source. Therein, narrow-linewidth lasers increase the number of information channels that can be encoded as constellations in the complex plane of the field amplitude [2, 3]. In yet another example, the lowest, close-to-carrier phase-noise microwave signals are now derived through frequency division of a high-coherence laser source using an optical comb as the

#171557 - $15.00 USD Received 2 Jul 2012; revised 10 Aug 2012; accepted 12 Aug 2012; published 20 Aug 2012

frequency divider [1]. The miniaturization of these all-optical microwave oscillators could provide a chip-based alternative to electrical-based microwave oscillators, but with unparalleled phase noise stability. Moreover, with the advent of microcombs [7, 8], such an outcome seems likely provided that similar strides are possible in miniaturization of high-coherence sources and reference cavities. Typically, however, miniaturization comes at the expense of coherence, because quantum and technical noise contributions to laser coherence increase as laser-cavity form factor is decreased. Recently, however, there has been remarkable progress in achieving highly coherent, compact laser sources. Both Erbium and Raman microlasers with short-term, Schawlow-Townes linewidths in the range of 10 Hz have been reported [9, 10]. Also, a fully packaged narrow linewidth laser that uses feedback from an ultra-high-Q resonator to a semiconductor laser has also been demonstrated [11].

Recently, we reported a stimulated Brillouin laser that attains a high level of coherence and is based on a new, ultra-high-Q resonator fabricated from silica on silicon [12]. Schawlow-Townes noise of 0.06 Hz^2/Hz is measured at an output power of approximately 400μW. Also significant is that the low-frequency technical noise is comparable to commercial fiber lasers. In the present work, we explore further details of this laser's operation including mode-pulling phenomena, cascaded operation, and a study of the Schawlow-Townes linewidth for the Brillouin laser. Concerning the latter, while conventional (inversion-based) optical lasers feature a Schawlow-Townes noise that is immune from thermal quanta, Brilluoin lasers, on account of coupling to the mechanical bath, feature a significant mechanical noise contribution to the laser phase noise. We both derive this contribution and use the theory to extract the thermal quanta contribution from data. Finally, the potential application of these devices as spectral purifiers for lower coherence lasers is discussed.

2. Lithographic fabrication of Brillouin lasers

Stimulated Brillouin scattering has been used to create narrow-linewidth fiber lasers [13] and to study slow light phenomena [14] in optical fiber. However, on account of the challenge in matching the Brillouin shift to a pair of cavity modes, only recently have the first microcavity-based SBLs been demonstrated. These devices leverage a high spectral density of transverse modes in CaF_2 [15] or microsphere resonators [16] to create a reasonable likelihood of frequency matching. Even more recently, chalcogenide waveguides have been used to achieve Brillouin oscillation [17]. In the present work, control of the resonator diameter using a new ultra-high-Q resonator geometry [12] is applied to precisely match the free spectral range (FSR) to the Brillouin shift. The resonators attain Q factors as high as 875 million [12], even exceeding the performance of microtoroids [18]; and significantly, they are fabricated entirely from standard lithography and etching. The combination of ultra-high-Q and precision control of FSR has not previously been possible, and is essential for reliable fabrication of low-threshold, microcavity-based, SBL lasers. Moreover, the same issue that has made SBL devices so difficult to fabricate in microcavity form (the relatively narrow gain spectrum) becomes an asset in attaining highly stable, single-line laser oscillation.

Very briefly, the fabrication of these devices uses an 8-10 micron thick thermal oxide layer that is lithographically patterned and etched into circular disks using buffered HF. The etched, oxide disks then act as a mask for selective, dry-etching of the silicon. This dry etch process creates a whispering gallery resonator through undercut of the silicon. By proper control of both the wet and dry etching processes, the Q of the resulting resonator can be nearly 1 billion. Moreover, the lithography and etching process provide diameter control of 1:20,000, giving only 0.5 MHz of FSR uncertainty for a cavity of 10 GHz FSR. This level of control is more than sufficient to place the microcavity FSR within the Brillouin frequency shift. Figure 1(b) shows a top view of a resonator fabricated using this procedure. Additional details on fabrication and

#171557 - $15.00 USD Received 2 Jul 2012; revised 10 Aug 2012; accepted 12 Aug 2012; published 20 Aug 2012

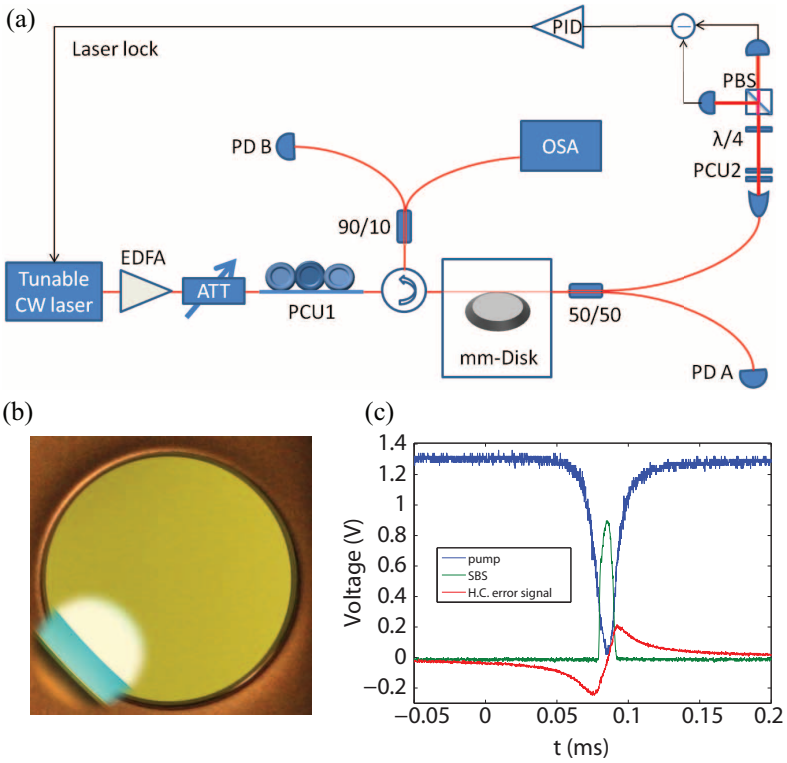

Fig. 1. **Experimental setup.** (a) A tunable CW laser is amplified through an EDFA and coupled into the disk resonator using the taper-fiber technique. The SBL emission in the backward direction propagates through the fiber circulator, and is monitored by a photodetector (PD B) and an optical spectrum analyzer (OSA). The pump is monitored by a separate photodetector (PD A) and is also coupled to a balanced-homodyne detection setup (Hänsch-Couillaud technique) to generate an error signal for locking the pump laser to the cavity resonance. (b) A micrograph of the SBL disk resonator used in this experiment. The disk has a diameter of approximately 6.02 mm. (c) Experimental oscilloscope traces for transmitted pump, back-propagating SBL and Hänsch-Couillaud error signal.

characterization of these resonators are described in [12].

3. Cascaded versus single-line Brillouin laser action

Figure 1(a) shows the experimental setup used to test the SBLs. Pump power is coupled into the resonator by way of a fiber taper coupler [19, 20]. SBL emission is coupled into the opposing direction and routed via a circulator into a photodiode and an optical spectrum analyzer. The transmitted pump wave is monitored using a balanced homodyne receiver so as to implement a Hänsch-Couillaud locking of the pump to the resonator [21, 22]. Figure 1(c) shows the typical experimental traces for the transmitted pump, back-propagating SBL and the Hänsch-Couillaud error signal as the pump laser is scanned across the microcavity resonance.

By proper control of taper loading, the SBL can be operated in two distinct ways: cascade or single-line. Figure 2(a) shows the optical spectrum of a single-line SBL and Fig. 2(b) shows the spectrum for cascaded operation up to the 9th order. In cascade, the waveguide loading is kept low so that once oscillation on the first Stokes line occurs, it can function as a pump wave for a

#171557 - $15.00 USD Received 2 Jul 2012; revised 10 Aug 2012; accepted 12 Aug 2012; published 20 Aug 2012

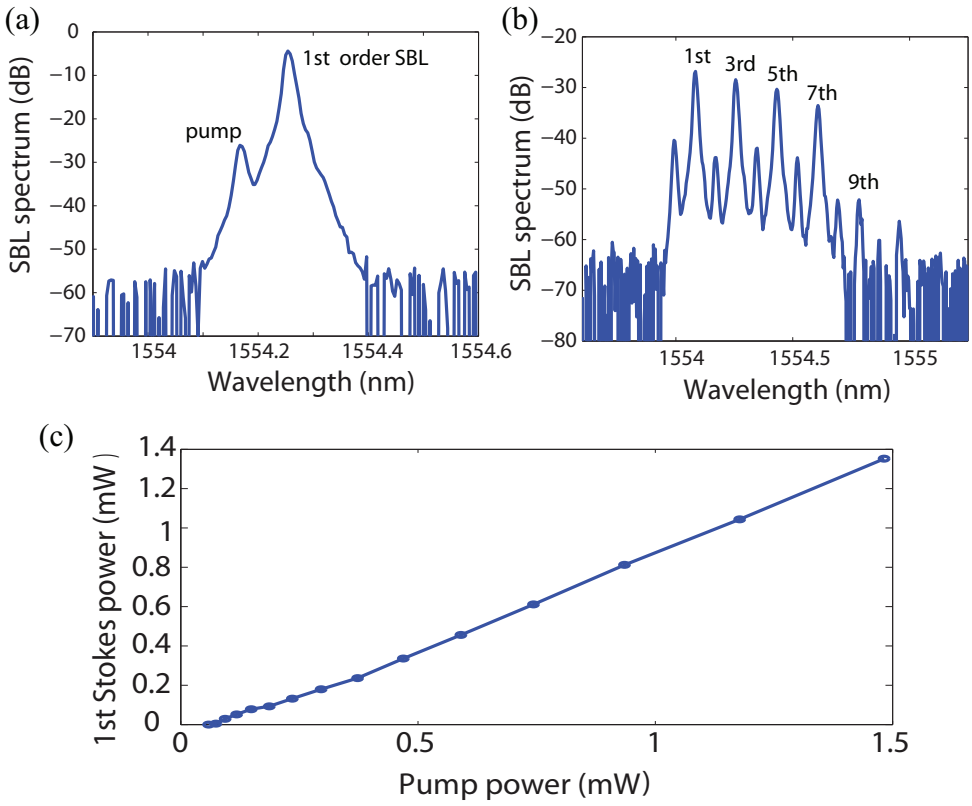

Fig. 2. **SBL optical spectra and output power versus pump power for single-line operation.** (a) A spectrum showing single-line SBL operation wherein only the 1st-order emission line is excited. (b) Spectrum showing cascaded SBL operation up to the 9th order. In both figures, the spectrum is collected in the backward direction with the pump and even order SBL emission lines suppressed on account of their propagation in the forward direction (i.e., the observed, weak level for these signals in the spectrum is a result of weak back-reflection in the experimental setup). (c) Output power of the 1st-order Stokes wave while adjusting the cavity loading so as to maintain critical coupling in each step. The differential efficiency is around 95%.

second Brillouin wave and so on. Single-line operation, on the other hand, is often desirable in system applications [1–3] and can be obtained by increasing the resonator waveguide coupling. While cascading can still be made to occur at a sufficiently high pumping power, increased waveguide loading forestalls this process by increasing the oscillation threshold. Significantly, there is no penalty in efficiency as a result of the increased waveguide loading. Indeed, because the internal loading on the pump rises with increased Stokes power, one can preset the waveguide loading to an over-coupled condition such that the pump wave will become critically coupled only at the desired Stokes power. Alternately, in cases where waveguide coupling can be varied, the coupling can be adjusted so as to always achieve critical coupling of the pump as the 1st-Stokes wave increases in power. Figure 2(c) shows just this scenario. The power of the 1st-order Stokes laser line is plotted versus the pump power with the cavity loading adjusted to maintain critical coupling in each step. A linear relationship is obtained and the differential pumping efficiency is 95%.

#171557 - $15.00 USD Received 2 Jul 2012; revised 10 Aug 2012; accepted 12 Aug 2012; published 20 Aug 2012

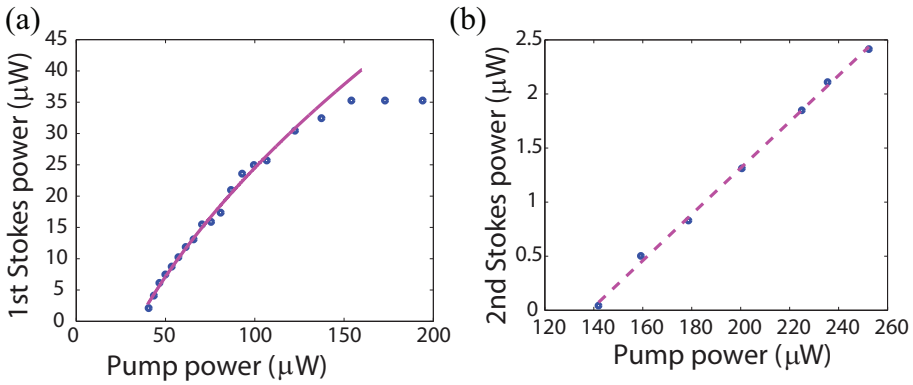

Fig. 3. **SBL output power dependence on pump power in cascaded operation.** (a) Experimental output power of the 1st-order SBL versus the pump power. A threshold of 40 μW is obtained. The output power of the 1st-order SBL is clamped for pump power above 150 μW because the 2nd-order SBL begins oscillation. Also shown is the fitted curve using $P_{th}\left(\sqrt{\frac{P_{pump}}{P_{th}}}-1\right)$. (b) Experimental output power of the 2nd-order SBL versus the pump power. Also shown is the linear fit with respect to the pump power.

It is also interesting to measure the dependence of the different SBL Stokes emission lines with respect to the pump power. It was shown in [23, 24] that for stimulated Raman scattering from a UHQ toroid cavity, the 1st-order Raman Stokes power scales with the square root of the pump power while the 2nd-order Stokes power scales linearly with the pump power (given a fixed taper-fiber coupling condition). The stimulated Brillouin laser in this work satisfies quite similar laser rate equations as the stimulated Raman laser in [23, 24]. Thus, similar pump-power dependences of the different Stokes lines are expected for the SBL. Figure 3(a) shows the output power of the 1st-order Stokes line versus pump power with the cavity loading fixed, and also a curve fitting using $P_{th}\left(\sqrt{\frac{P_{pump}}{P_{th}}}-1\right)$. The flattening of the 1st-order power for pump power exceeding 150 μW results from the onset of threshold for the 2nd-order Stokes line. On account of gain clamping, the 1st-order Stokes line (now acting as the pump wave for the 2nd-order Stokes laser oscillation) experiences circulating power clamping beyond this power. Figure 3(b) shows the output power of the 2nd-order Stokes emission versus input pump power with the cavity loading fixed. The linear dependence is, again, consistent with observations reported earlier for cascaded Raman laser action.

4. Frequency pulling in the SBL

Frequency/mode pulling in a conventional laser oscillator is well studied. In a laser having an atomic gain medium, the atomic dispersion modifies the round-trip phase of the intra-cavity field and "pulls" the laser oscillation frequency from the passive cold cavity value towards that of the atomic resonance [25]. The Brillouin gain can also introduce dispersive phase shift inside the microcavity. Recently, mode pulling in a fiber Brillouin laser was accounted for to explain frequency tuning range under a novel strain tuning mechanism [26]. However, to the authors' knowledge there has never been a quantitative measurement of mode pulling in Brillouin lasers.

To model the pulling, we introduce a pump field, A (frequency ω_p), 1st-order Stokes field, a (frequency ω_s), with corresponding "cold cavity" resonant frequencies ω_0 and ω_1. The fields are normalized so that their square modulus gives the photon number in the cavity. They satisfy

#171557 - $15.00 USD Received 2 Jul 2012; revised 10 Aug 2012; accepted 12 Aug 2012; published 20 Aug 2012

the following equations of motion:

$$\dot{A_o} = [i(\omega_p - \omega_0) - \gamma/2]A_o + i\sqrt{\gamma_{ex}}s - g^c|\alpha|^2 A_o \tag{1}$$

$$\dot{\alpha} = [i(\omega_s - \omega_1) - \gamma/2]\alpha + g^c|A_o|^2\alpha \tag{2}$$

$$g^c = \frac{g_0^c}{1 + \frac{2i[\omega_p - \omega_s - \Omega]}{\Gamma}} = \frac{g_0^c(1 - \frac{2i\Delta\Omega}{\Gamma})}{1 + \frac{4\Delta\Omega^2}{\Gamma^2}} \tag{3}$$

where A_o and α are the slowly varying amplitudes for the pump and the stokes fields, $\Delta\Omega = \omega_p - \omega_s - \Omega$, and Γ is the full-width half maximum linewidth of the Brillouin gain. Ω is the Brillouin shift frequency, which depends on the pump wavelength λ_p according to $\Omega/2\pi = \frac{2nV_A}{\lambda_p}$, n is the refractive index of silica and V_A is the acoustic velocity in silica. Also, γ is the photon damping rate of the loaded cavity, and γ_{ex} is the waveguide coupling rate. s is the input pump field amplitude, normalized such that $|s|^2$ gives the incident photon rate. (As an aside, Eq. (3) is valid in the limit that the Brillouin linewidth is narrower than the Brillouin shift. This condition is satisfied in the present system.)

The real part of Eq. (3) gives the Brillouin gain spectrum with Lorentzian line shape and the imaginary part is dispersive component that will "pull" the Brillouin oscillation frequency. Steady state solution of these equations yields the following pair of equations,

$$|A_o|^2 = \frac{\gamma}{2}\frac{1 + \frac{4\Delta\Omega^2}{\Gamma^2}}{g_0^c} \tag{4}$$

$$\omega_s - \omega_1 - \frac{g_0^c \frac{2\Delta\Omega}{\Gamma}}{1 + \frac{4\Delta\Omega^2}{\Gamma^2}}|A_o|^2 = 0 \tag{5}$$

Equation (4) gives the threshold intra-cavity pump photon number. Equation (5) is the frequency pulling equation. Substituting Eq. (4) into Eq. (5) gives the 1st-order Stokes lasing frequency ω_s. In the experiment, the beat frequency between the pump and 1st-Stokes wave is measured ($\Delta\omega_{beat} = \omega_p - \omega_s$) and this is given by the following expression,

$$\Delta\omega_{beat} = \frac{1}{1 + \frac{\gamma}{\Gamma}}(\Delta\omega_{FSR} + \frac{\gamma}{\Gamma}\Omega) \tag{6}$$

where $\Delta\omega_{FSR} = \omega_0 - \omega_1$ is the cold cavity free spectral range. Usually, $\Gamma \approx 2\pi\times$ (20 - 60) MHz for silica waveguides. Also, $\gamma \approx 2\pi\times 1$ MHz in our cavity so that $\gamma \ll \Gamma$. Under these conditions, Eq. (6) can be approximated in the following form,

$$\Delta\omega_{beat} - \Delta\omega_{FSR} = \frac{\gamma}{\Gamma}(\Omega - \Delta\omega_{FSR}) \tag{7}$$

where $\Delta\omega_{beat} - \Delta\omega_{FSR} = \omega_1 - \omega_s$ is the frequency pulling caused by Brillouin dispersion. Note that the effect of this equation is to pull the Stokes lasing frequency towards the line center of the Brillouin gain (in analogy to the atomic resonance in conventional laser systems). Moreover, when the FSR matches the Brillouin shift, the frequency pulling is zero.

Figure 4 summarizes the experimental results of the frequency pulling study. In this measurement, the pump wavelength is sequentially tuned along the cavity modes within the same mode family. The SBL threshold, cold-cavity FSR and Brillouin beat frequency are measured at each wavelength. Also plotted are the linear fits to the cold cavity FSR and Brillouin beat as well as quadratic fit to the threshold power. Considering the threshold behavior first, the quadratic fitting of the threshold power is in agreement with Eq. (4). The minimum threshold corresponds to

#171557 - $15.00 USD Received 2 Jul 2012; revised 10 Aug 2012; accepted 12 Aug 2012; published 20 Aug 2012

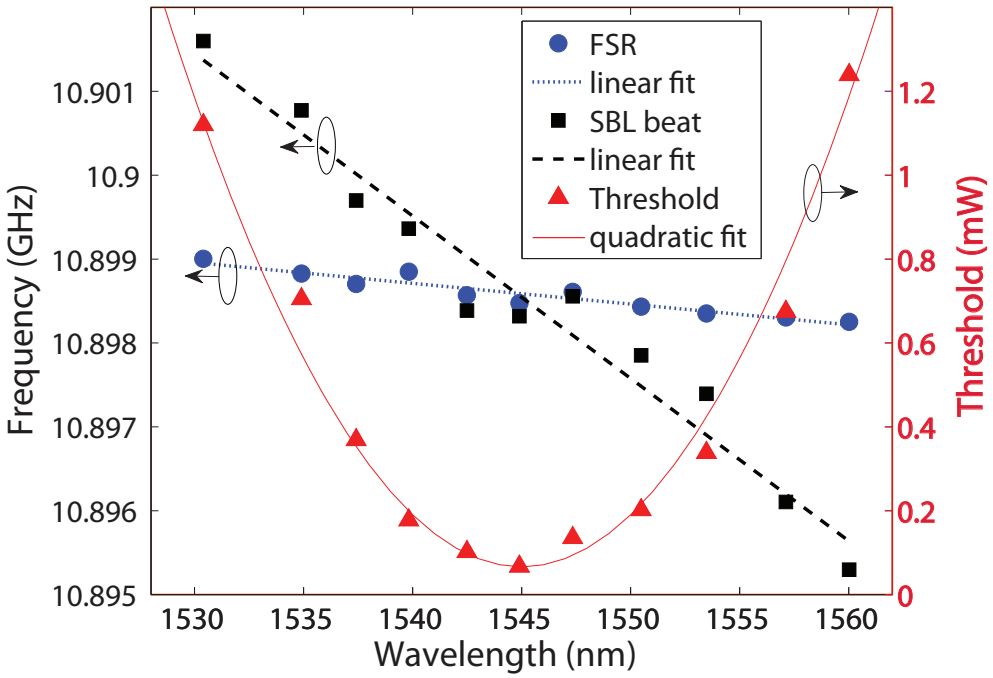

Fig. 4. **SBL mode pulling measurement.** The measured cold cavity FSR (circles), Brillouin beat frequency (squares) and SBL threshold power (triangles) are plotted versus the pump wavelength. The linear fit of the cold cavity FSR gives a slope of $-2\pi\times$ 0.02 MHz/nm and the fit of the Brillouin beat frequency gives a slope of $-2\pi\times$ 0.19 MHz/nm. The quadratic fit of the threshold power yields the Brillouin gain linewidth of $2\pi\times$ 51 MHz.

excitation at the peak of the Brillouin Lorentzian gain spectrum (i.e. the cold cavity FSR = Brillouin shift), and the rise of the threshold corresponds to excitation at frequency detunings that are progressively further away from the gain peak. It is easily shown that $\frac{d\Omega}{d\lambda_p} = -\frac{\Omega}{\lambda_p} = -2\pi\times$ 7 MHz/nm [12], meaning that 1nm increase of the pump wavelength will decrease the Brillouin shift by 7 MHz. Thus, from the quadratic fit, the Brillouin gain bandwidth is estimated to be $\Gamma = 2\pi\times$ 51 MHz. The cavity mode has intrinsic Q of 300 million , giving a corresponding value for $\gamma/2\pi$ of 1.29 MHz at critical coupling . Thus from Eq. (7), where all terms depend on λ_p, the frequency pulling coefficient $\frac{d\Delta\omega_{beat}}{d\lambda_p}$ is estimated to be $-2\pi\times$ 0.20 MHz/nm. The linear fit in Fig. 4 gives $\frac{d\Delta\omega_{beat}}{d\lambda_p} = -2\pi\times$ 0.19 MHz/nm (and $\frac{d\Delta\omega_{FSR}}{d\lambda_p} = -2\pi\times$ 0.02 MHz/nm). The theoretical and experimental pulling rates are therefore in good agreement.

5. Fundamental linewidth of stimulated Brillouin laser

The Hamiltonian for parametric coupling of a mechanical field, b (frequency Ω), and a Stokes field, a (frequency ω_1), that is induced by a pump field $A(t)$ (via matrix element μ) is given by [27–29]:

$$H = \hbar\omega_1 a^\dagger a + \hbar\Omega b^\dagger b + \frac{\hbar\mu}{2}\left(A(t)^* ba + A(t)a^\dagger b^\dagger\right).$$

#171557 - $15.00 USD Received 2 Jul 2012; revised 10 Aug 2012; accepted 12 Aug 2012; published 20 Aug 2012

where this Hamiltonian omits energy non conserving terms. Introducing slowly varying operators for the Stokes and the mechanical fields, and also treating the blue pump mode as a classical, non-dynamical field, the relevant equations of motion are:

$$\dot{\beta}^{\dagger} = -\frac{\Gamma}{2}\beta^{\dagger} + i\frac{\mu}{2}A_o^{*}\alpha e^{i\Delta\Omega t} + F(t) \tag{8}$$

$$\dot{\alpha} = \left[i(\omega_s - \omega_1) - \frac{\gamma}{2}\right]\alpha - i\frac{\mu}{2}A_o\beta^{\dagger}e^{-i\Delta\Omega t} + f(t) \tag{9}$$

where α and β are the slowly varying operator fields for the Stokes and the mechanical fields; Γ (γ) is the mechanical (optical) energy decay rate, $\Delta\Omega = \omega_p - \omega_s - \Omega$, and where $F(t)$ and $f(t)$ are Langevin operators with the standard normalization for damped oscillators [30,31]. We now restrict the solution of these equations to a regime in which the mechanical field is much more strongly damped than the optical field. This is a case typical of the devices considered in this study. The resulting adiabatic elimination of the more strongly-damped field results in corresponding amplification of the other, less-strongly damped field. In the regime ($\gamma \ll \Gamma$) elimination of β gives:

$$\dot{\alpha} = \left[i(\omega_s - \omega_1) - \frac{\gamma}{2}\right]\alpha + g^c|A_o|^2\alpha + h(t)$$

where g^c is the gain parameter introduced in the discussion of frequency pulling and is related to the matrix element μ by $g_0^c = \mu^2/2\Gamma$. $h(t)$ is fluctuation operator that depends upon the original operators introduced in Eqs. 8 and 9. As an aside, the adiabatic approximation applied in this analysis eliminates the possibility of contributions from the optical pump to the SBL phase noise. These contributions have been studied in Brillouin fiber ring lasers [32, 33] and also analyzed in the first reports of SBS laser action in microresonators (see Eq. (4) in [15]). They are suppressed by a factor $(1+\Gamma/\gamma)^2$ or about 2000X in the current device. Nonetheless, they are interesting and potentially important in cases where pumps have large amounts of phase noise. In the current study, there was no evidence of these fluctuations in the Schawlow-Townes noise spectrum discussed below.

Analysis of the phase noise in the Stokes field using the standard approach gives the following linewidth formula:

$$\Delta\nu = \frac{\gamma}{4\pi N_S}(n_T + N_T + 1) \tag{10}$$

where $\Delta\nu$ is the laser linewidth in Hertz. Also, $\bar{N}_S$ and N_T are the number of coherent and thermal quanta in the Stokes field while n_T is the number of thermal quanta in the mechanical field. N_T is negligible at optical frequencies and has been included here only to indicate the symmetrical form of thermal noise contributions from the optical and mechanical degrees of freedom. The unity term in the expression is of quantum origin, and results from the two underlying degrees of freedom (optical and mechanical oscillator fields) each contributing 1/2 to the zero point (in addition to the already noted thermal occupancy). The cumulative contribution from these two sources provides the unity in the above expressions. It is also interesting to note that based upon analysis in [15] we would expect a small correction factor to Eq. (10) of the form $(1+\gamma/\Gamma)^{-2}$ resulting from the adiabatic approximation made above. This correction would be of order of a few percent using the system parameters.

The above form of the linewidth can be rewritten in terms of more-readily-measurable quantities as follows:

$$\Delta\nu = \frac{\hbar\omega^3}{4\pi P Q_T Q_E}(n_T + N_T + 1) \tag{11}$$

#171557 - $15.00 USD Received 2 Jul 2012; revised 10 Aug 2012; accepted 12 Aug 2012; published 20 Aug 2012

where $Q_{T,E}$ are the total and external Q factors, and P is the output power of the Brillouin laser. In this form, the expression is similar to the Schawlow-Townes formula for an inversion-based laser. In comparing this formula to the conventional Schawlow-Townes formula, the presence of the mechanical thermal quanta (as well as their zero-point contribution) is new and alters the magnitude of the linewidth. In the present case of Brillouin oscillation near a mechanical frequency of 10.8 GHz, $n_T = 569$ and this factor greatly increases the value of the linewidth over its vacuum-noise-limited value.

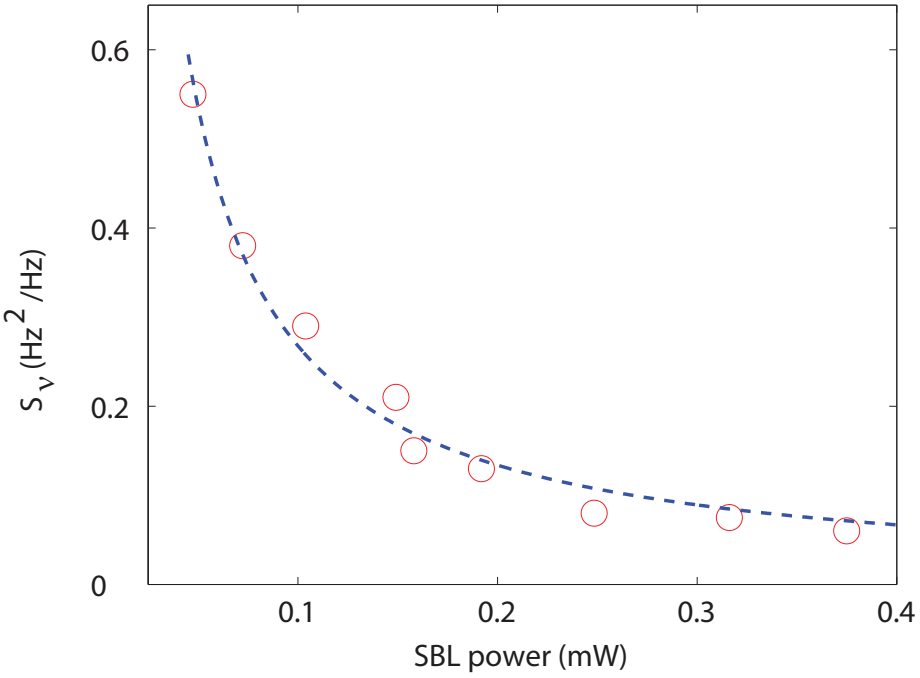

Fig. 5. **Measurements of the SBL Schawlow-Townes-like, frequency noise characteristics** (Original data appeared in the supplemental information of [12]). The dashed line is an inverse power fit to the data.

The Schawlow-Townes-like noise of this device has been reported in [12] and that data is reproduced in Fig. 5. Briefly, to characterize this frequency noise, a Mach-Zehnder interferometer having a free spectral range of 6.72 MHz is used as a discriminator and the transmitted optical power is detected and measured using an electrical spectrum analyzer (ESA). The white noise portion of the resulting spectrum can then be measured and plotted as a function of output power. Figure 5 shows this data and also an inverse power curve fitting according to Eq. (11). The thermal quanta of the mechanical field can be derived from the measurement values of the ST noise levels. For the device in the measurement, Q_T = 140 million, Q_E = 390 million, which gives $n_T \approx 600$. This is in good agreement with the theoretical thermal quanta value at room temperature (569). The minimum value of 0.06 Hz^2/Hz for the Schawlow-Townes noise is to our knowledge the lowest recorded ST noise for any chip-based laser.

#171557 - $15.00 USD Received 2 Jul 2012; revised 10 Aug 2012; accepted 12 Aug 2012; published 20 Aug 2012

6. Discussion and conclusion

The combined effect of adiabatic suppression of pump noise and very low Schawlow-Townes noise means that the SBL device studied here acts as a spectral purifier, boosting the coherence of the pump wave. The relatively small frequency shift created in this process (about 11 GHz) can be easily compensated. For example, low coherence DFB lasers are manufactured with wavelengths set on the ITU grid by control of an integrated grating pitch with fine-control provided by temperature tuning of the fully packaged device. A DFB laser could be tuned through this same process to function as an SBL pump so that the emitted SBL wavelength resides at the desired ITU channel. In this way, the existing WDM infrastructure could be adapted for high-coherence operation in optical QAM systems. The frequency noise levels demonstrated here exceed even state of the art monolithic semiconductor laser by 40dB [34]. Using the measured phase noise, it is estimated that Square 1024-QAM formats could be implemented using an SBL generated optical carrier at 40GB/s.

While the current devices use a taper coupling for launch of the pump and collection of laser signal, the ability to precisely control the resonator boundary enables use of microfabricated waveguides for this process. Several designs are under investigation, the implementation of which will extend the range of applications of the SBL devices. For example, the SBLs demonstrated here are candidates for locking to a reference cavity so as to create Hertz or lower long-term linewidths. Such a source on a chip might one day be combined with microcomb technology [8] to realize a compact and high-performance microwave oscillator. At the tabletop scale, these comb-based systems have recently exceeded the performance of cryogenic electronic oscillators [1]. Also, another approach for stable, microwave generation relies upon heterodyne mixing of stable Brillouin laser lines in optical fiber [35]. The present devices would be interesting candidates for this same approach.

In conclusion, we have characterized single-line and cascaded operation up to the 9th-order in a novel chip-based Brillouin laser. Moreover, a technique for controllable operation with or without cascade has been demonstrated. Frequency pulling induced by the SBS nonlinear phase shift has been modeled and observed. A theoretical formula for the foundamental linewidth of the SBL has been derived and we have used it to show that the thermal quanta of the mechanical mode greatly enhances the Schawlow-Townes noise of the SBL. Existing data on ST noise has been analyzed using this model to infer a value for the thermal quanta in the mechanical mode of the present laser system. The inferred value is in good agreement with the theory of a mechanical mode in thermal equilibrium. Finally, the SBL in this work features the lowest fundamental linewidth recorded for any chip-based laser.

Acknowledgments

The authors would like to acknowledge helpful discussions with Scott Diddams and Scott Papp. The authors are also grateful for financial support from the DARPA ORCHID program, the Institute for Quantum Information and Matter, an NSF Physics Frontiers Center with support of the Gordon and Betty Moore Foundation, and the Kavli NanoScience Institute.

#171557 - $15.00 USD Received 2 Jul 2012; revised 10 Aug 2012; accepted 12 Aug 2012; published 20 Aug 2012